Available online at www.sciencedirect.com
SCIENCE DIRECT®
Journal of Inorganic Biochemistry 98 (2004) 1837–1850
JOURNAL OF Inorganic Biochemistry
www.elsevier.com/locate/jinorgbio

Inhibition of yeast growth by molybdenum-hydroxylamido complexes correlates with their presence in media at differing pH values

Debbie C. Crans [a,*], Jason J. Smee [a], Edita G. Gaidamauskiene [a], Oren P. Anderson [a], Susie M. Miller [a], Wenzheng Jin [a], Ernestas Gaidamauskas [a,b], Etienne Crubellier [a], Rose Grainda [a], Lai-Har Chi [c], Gail R. Willsky [c]

[a] *Department of Chemistry, Colorado State University, Fort Collins, CO 80523-1872, USA*
[b] *Faculty of Chemistry, Vilnius University, Naugarduko 24, Vilnius LT-03225, Lithuania*
[c] *Department of Biochemistry, University at Buffalo, School of Medicine and Biomedical Sciences, 140 Farber Hall, Buffalo, NY 14214, USA*

Received 21 February 2004; received in revised form 12 July 2004; accepted 17 August 2004
Available online 15 September 2004

Abstract

The effects of Mo-hydroxylamido complexes on cell growth were determined in *Saccharomyces cerevisiae* to investigate the biological effects of four different Mo complexes as a function of pH. Studies with yeast, an eukaryotic cell, are particularly suited to examine growth at different pH values because this organism grows well from pH 3 to 6.5. Studies can therefore be performed both in the presence of intact complexes and when the complexes have hydrolyzed to ligand and free metal ion. One of the complexes we examined was structurally characterized by X-ray crystallography. Yeast growth was inhibited in media solutions containing added Mo-dialkylhydroxylamido complexes at pH 3–7. When combining the yeast growth studies with a systematic study of the Mo-hydroxylamido complexes' stability as a function of pH and an examination of their speciation in yeast media, the effects of intact complexes can be distinguished from that of ligand and metal. This is possible because different effects are observed with complex present than when ligand or metal alone is present. At pH 3, the growth inhibition is attributed to the forms of molybdate ion that exist in solution because most of the complexes have hydrolyzed to oxomolybdate and ligand. The monoalkylhydroxylamine ligand inhibited yeast growth at pH 5, 6 and 7, while the dialkylhydroxylamine ligands had little effect on yeast growth. Growth inhibition of the Mo-dialkylhydroxylamido complexes is observed when a complex exists in the media. A complex that is inert to ligand exchange is not effective even at pH 3 where other Mo-hydroxylamido complexes show growth inhibition as molybdate. These results show that the formation of some Mo complexes can protect yeast from the growth inhibition observed when either the ligand or Mo salt alone are present.

Keywords: Molybdenum complex; *N*-Alkylhydroxylamine; Yeast; Solution chemistry; Crystal structure; pH effects on growth; Intact complex

1. Introduction

Labile metal complexes are presumed to have the same effect on cell growth as that of the metal salt and ligand. In this work, we investigate the effects of a series of four molybdenum (Mo) complexes on yeast growth as a function of compound structure and pH. Mo is a transition metal that has a biological function as a metal ion cofactor in many Mo-containing enzymes. Molybdate is commonly used as a nutritional supplement and Mo is readily absorbed in humans.

* Corresponding author. Tel.: +19704917635; fax: +19704911801.
E-mail address: crans@lamar.colostate.edu (D.C. Crans).

0162-0134/$ - see front matter © 2004 Elsevier Inc. All rights reserved.
doi:10.1016/j.jinorgbio.2004.08.010

The recommended daily allowance (RDA) for this ultratrace element in adults is 0.78–2.61 μmol [1] or 75–250 μg [2]. It is a relatively non-toxic element, with an intake of 1–52 mmol Mo/kg of food or water needed to produce clinical symptoms [1]. The simple Mo salt, sodium molybdate, has been found to lower diabetic hyperglycemia in both diabetic rats and mice [3,4] and to affect glucose metabolism in isolated hepatocytes [5]. A study comparing molybdenum uptake in *Saccharomyces cerevisiae* and *Candida krusei* yeast cells, showed that molybdate is accumulated by *S. cerevisiae*, but not by *C. krusei* [6]. More than 80% of the Mo present in the medium was found to be cell-associated in *S. cerevisiae*, which is in marked contrast to *C. krusei* where less than 1% of the Mo was cell-associated. Since Mo is a relatively non-toxic metal ion which forms labile metal complexes and the beneficial modes of action of Mo compounds in alleviating some of the symptoms of diabetes are not well understood, more information correlating the effects of Mo compounds on cellular systems is of interest.

Mo complexes with hydroxylamido ligands were chosen for these studies, in part because of the known chemistry of representative simple complexes [7–22], and in part because of their anticipated analogy with their corresponding vanadium-hydroxylamido complexes [16,19,23–25]. The most common bonding modes for hydroxylamines are the end-on and the bidentate modes. The simple mono- and dialkylhydroxylamido Mo complexes $[MoO_2(MeHNO)_2]$ (**1**), $[MoO_2(Me_2NO)_2]$ (**2**) and $[MoO_2(Et_2NO)_2]$ (**3**) have the MoO_2 unit coordinated to two bidentate hydroxylamido ligands to give a distorted six-coordinate geometry [16,17]. The structure of these complexes is similar to that of the simple peroxo derivatives, which tend to be six-coordinate mononuclear or seven-coordinate dinuclear complexes [26]. Herein we report an X-ray structure of complex **2**, which is the third example from this simple class of Mo-hydroxylamido compounds to be structurally characterized in the solid state.

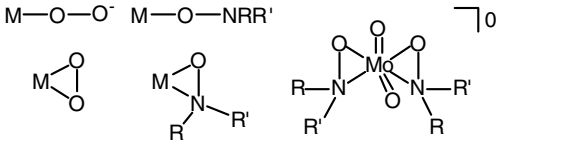

R = H, R' = Me, $[MoO_2(MeHNO)_2]$ (1)
R = R' = Me, $[MoO_2(Me_2NO)_2]$ (2)
R = R' = Et, $[MoO_2(Et_2NO)_2]$ (3)

The aqueous chemistry of hydroxylamido complexes is generally limited to a narrow pH range near neutral pH (vide infra). In addition to their hydrolytic chemistry, many hydroxylamido complexes also undergo redox and insertion-type reactions [27]. We have not investigated the parent hydroxylamine (H_2NOH), because it is readily oxidized by some transition metal ions to form nitric oxide (NO) [27] and efforts to prepare the corresponding Mo(VI) complex always lead to NO complexes regardless of pH [27]. In contrast to the Mo-hydroxylamido complexes, the Mo(NO)-type complexes are very stable over a wide pH range. The type of mononitrosyl Mo complex we investigated in this study can be formally described as a Mo(II) complex, assuming NO has a charge of +1, or as a $\{Mo\text{-}NO\}^4$ complex according to the Enemark–Feltham notation [1] [28]. We have investigated the effects of a series of one Mo(NO)-hydroxylamido complex $[Mo(NO)(H_2NO)(H_2O)(dipic)]$, (**4**), and three simple Mo-alkylhydroxylamido complexes (**1**–**3**) on yeast growth as a function of pH to obtain fundamental information on cellular responses to labile transition metal complexes. The Mo-hydroxylamido complexes selected include one mono- and two dialkylated Mo-hydroxylamido complexes (**1**–**3**) and a hydrolytically stable Mo(NO)-type complex (**4**). Yeast was chosen as a model system because it is a good model of an eukaryotic cell. Furthermore, it grows well over a wide pH range, and allows one to determine the effect of complexes both when the compounds remain intact and when the compounds have hydrolyzed.

In order to interpret the growth effects observed in yeast, the stability of the complexes was studied in pure water; in addition, investigations were also undertaken at high ionic strength and in yeast media. In these studies, under the three different conditions, the amount of complex varied as a function of pH with the highest complex concentrations in the weakly acidic pH range. The effects of the compounds on yeast growth were determined over a wide pH range (pH 3, 5, 6, and 7), which covers conditions both where the majority of the complexes are intact (pH 5 and 6) and where most of the complexes have hydrolyzed (pH 3 and 7). The studies demonstrate that yeast growth is inhibited by the three Mo-hydroxylamido complexes (**1**–**3**) that can undergo ligand exchange at pH values where complex is present in media. An inert Mo complex containing one hydroxylamido group and one NO group (**4**) had no effect on growth. In conclusion, we observed that only Mo complexes that are capable of undergoing ligand exchange inhibit yeast growth and that the inhibition is manifested solely when the complex is present in the growth media.

[1] The notation is derived from the total number of d electrons, assuming that NO is a neutral ligand, and from the total number of π* electrons from all the NO ligands (one electron per NO). See [28] for examples.

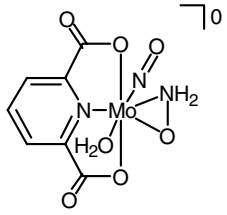

[Mo(NO)(H$_2$NO)(H$_2$O)(dipic)] (4)

2. Experimental

2.1. Materials

All chemicals used were of reagent grade. The water was distilled and deionized on an ion-exchange column. *N*-Methylhydroxylamine hydrochloride (MeHNOH · HCl) (Fluka), *N*,*N*-dimethylhydroxylamine hydrochloride ($Me_2NOH \cdot HCl$) (Fluka), *N*,*N*-diethylhydroxylamine (Et_2NOH) (85% w/w solution, Aldrich), 2,6-dipicolinic acid (H_2dipic) (Aldrich), 4-hydroxy-2,6-dipicolinic acid (H_2dipic-OH) (TCI America), $Na_2MoO_4 \cdot 2H_2O$ (Strem), $(NH_4)_6(Mo_7O_{24}) \cdot 4H_2O$ (Fisher), hydroxylamine hydrochloride ($H_2NOH \cdot HCl$) (Fisher) and H_2O_2 (30% w/w solution, Fisher) were used as received. NH_4[VO_2(dipic-OH)] was prepared as previously described [29]. The slightly off-white [$MoO_2(Et_2NO)_2$] (**3**) [2] was prepared as described previously [18]. The synthetic procedure was simplified as described below for the preparation of [$MoO_2(MeHNO)_2$] (**1**) [17] and [$MoO_2(Me_2NO)_2$] (**2**) [18]. The [Mo(NO)(H$_2$NO)(H$_2$O)(dipic)] (**4**) [30] and the [MoO(O_2)(H$_2$O)(dipic)] (**5**) [31] complexes were prepared as previously reported and their characterization was found to be satisfactory.

2.2. [$MoO_2(MeHNO)_2$] (*1*)

The compound was prepared using a slight modification of an earlier preparation [17]. To a stirred, 40 mL aqueous solution of $Na_2MoO_4 \cdot 2H_2O$ (7.20 g, 29.7 mmol) at 40 °C, was added solid MeHNOH · HCl (5.22 g, 62.5 mmol). After less than a min, a white precipitate formed and the mixture was cooled to ambient temperature and stirred for an additional 30 min. The white product was filtered off, washed with cold deionized water (3×10 mL) and diethyl ether (1×15 mL), and then dried overnight. A yield of 3.20 g (48.9%) was obtained. ^{1}H NMR (D_2O, ppm): 2.8 (s, 6H, –CH_3).

[2] ^{1}H NMR (D_2O, ppm): 3.1 (m, 8H, –CH_2–) 1.2 (t, 12H, –CH_3).

2.3. [$MoO_2(Me_2NO)_2$] (*2*)

An analogous procedure was followed for the preparation of [$MoO_2(Me_2NO)_2$] that avoids the *in situ* generation of Me_2NOH in the previous preparation [18]. An overall yield of 5.95 g (80.5%) of the white product was isolated. X-ray quality crystals were obtained by recrystallizing the compound from water. ^{1}H NMR (D^2O, ppm): 3.1 (s, 12H, –CH_3).

2.4. X-ray crystallography

X-ray diffraction data were recorded on a Bruker AXS SMART CCD diffractometer employing Mo Kα radiation (graphite monochromator). Crystallographic results and other details are listed in Table 1. An absorption correction was applied by using SADABS [32]. Structures were solved by direct methods and refined (on F_2, using all data) by a full-matrix, weighted least squares process. Anisotropic displacement parameters were used to refine all non-hydrogen atoms. Hydrogen atoms were placed in idealized positions. Standard Bruker control (SMART) and integration (SAINT) software were employed, and Bruker SHELXTL [33] software was used for structure solution, refinement and graphics.

Table 1
Crystal data and structure refinement for [$MoO_2(Me_2NO)_2$] (**2**)

Identification code	$MoO_2(Me_2NO)_2$
Empirical formula	$C_4H_{12}MoN_2O_4$
Formula weight	248.10
Temperature	173(2) K
Wavelength	0.71073 Å
Crystal system	Monoclinic
Space group	$P2_1/c$
Unit cell dimensions	a = 9.3008(12) Å, α = 90°
	b = 10.7140(14) Å, β = 100.089(2)°
	c = 9.2942(12) Å, γ = 90°
Volume	911.8(2) Å^3
Z	4
Density (calculated)	1.807 Mg/m^3
Absorption coefficient	1.414 mm^{-1}
F(000)	496
Crystal size	$0.10 \times 0.15 \times 0.18$ mm^3
θ range for data collection	3.43–23.26°
Index ranges	$-10 \leqslant h \leqslant 10$, $-11 \leqslant k \leqslant 11$,
	$-10 \leqslant l \leqslant 10$
Reflections collected	5589
Independent reflections	1307 [R_{int} = 0.0594]
Completeness to theta = 23.26°	99.5%
Absorption correction	SADABS
Refinement method	Full-matrix least-squares on F^2
Data/restraints/parameters	1307/0/101
Goodness-of-fit on F^2	0.960
Final R indices [$I > 2\sigma(I)$]	R_1 = 0.0296, wR_2 = 0.0896
R indices (all data)	R_1 = 0.0407, wR_2 = 0.0934
Extinction coefficient	0.012(2)
Largest difference peak and hole	0.519 and −0.384 e Å^{-3}

2.5. pH measurements

All pH measurements were done on an Orion 710A pH meter equipped with a Corning 476156-type combined glass electrode calibrated for H^+ ion concentration [34]. The measured pH values were accurate to within ± 0.05 units. For all D_2O-containing solutions the measured pH was corrected by subtracting 0.4 [35].

2.6. Electrochemical studies

Cyclic voltammetry was performed using a PARC model 173 potentiostat/galvanostat equipped with a PARC model 179 digital coulometer and employing a PARCH model 175 universal programmer. A three-electrode cell was used with a glassy carbon disk electrode (3.0 mm diameter) as the working electrode, a platinum wire as the auxiliary electrode and a Ag/AgCl reference electrode. The reference electrode was isolated from the main compartment and all potentials are reported vs. NHE (using Ag/AgCl = +0.222 V vs. the Normal Hydrogen Electrode, NHE). A solution of 2.0 mM $[Fe(CN)_6]^{3+}$ in 0.10 M $NaClO_4$ was used to calibrate the working electrode ($E_{Fe(III)/Fe(II)}$ = +0.356 V vs. NHE). Samples were prepared by dissolving the solid complex into an aqueous 0.1 M $NaClO_4$ solution. The pH values of the solutions were adjusted with 1.0 M $HClO_4$ or 1.0 M NaOH. The solutions were then purged with argon for 15 min prior to recording the cyclic voltammograms. All cyclic voltammograms were collected at a scan rate of 50 mV/s; the sweep ranges varied for each compound and covered the entire potential range possible before water decomposition.

2.7. NMR spectroscopic studies

2.7.1. Speciation

The solution samples for ^1H NMR measurements were prepared by dissolving either crystalline solid complex or ligand and $Na_2MoO_4 \cdot 2H_2O$ in D_2O. The solutions from pure complex (2.5 mM) were prepared in the pH range 3.0–7.0. The solutions prepared from molybdate and ligand consisted of a range of molybdate concentrations (1–10 mM) with ligand concentrations ranging from 1 to 100 mM, and the pH ranging from 2 to 10. Most studies used for the speciation calculations were carried out at 2.5 mM molybdate with 1–50 mM ligand. Specifically, in the $[MoO_2(Me_2NO)_2]$ system, the concentration dependent study was carried out at pH 5.7 and the amounts of Me_2NOH added were 1.0, 1.5, 2.0, 2.5, 5.0, 7.5, 10.0, 12.5, 15.0, 17.5, 20.0, 25.0 and 50.0 mM. The pH of the solution was adjusted using a stock solution of DCl or NaOD. The ^1H spectra were recorded on a Varian INOVA-400 spectrometer using standard parameters. Sodium 3-(trimethylsilyl)propane sulfonate (DSS) was used as an external reference for ^1H chemical shifts. Generally three separate, independent measurements were done. Each sample was prepared, measured and analyzed in triplicate and the errors reflect the means ± SD. Concentrations of the complexes were calculated from integrations of the complex and ligand signals in the samples' spectra; each spectrum was reintegrated using the Varian software to assure that the analysis, particularly in the presence of large amounts of excess ligand, gave consistent results.

The speciation calculations were done using the HySS program developed by Gans et al. [36]. The aqueous molybdate speciation and formation of oligomeric molybdates was assumed as described previously [37] with the following formation constants: $[HMoO_4]^-$ ($10^{3.39}$); $[Mo(OH)_6]$ ($10^{7.16}$); $[HMo_2O_7]^-$ ($10^{14.81}$); $[Mo_7O_{24}]^{6-}$ ($10^{52.8}$); $[HMo_7O_{24}]^{5-}$ ($10^{57.45}$) $[H_2Mo_7O_{24}]^{4-}$ ($10^{60.77}$); and $[Mo_8O_{26}]^{4-}$ ($10^{71.53}$).

2.7.2. Reaction with thiols

Stock solutions of 10–20 mM 2-mercaptoethanol and complex were prepared by dissolving pure compounds in D_2O, which were then thoroughly deoxygenated with an argon purge for at least 2 h. Solution pH was adjusted to 5.0 ± 0.2 or 7.0 ± 0.2 using NaOD and DCl solutions, and when necessary the pH was readjusted. Samples for analysis contained 2–5 mM of thiol and 2–5 mM of complex, and were prepared under an argon atmosphere and transferred into NMR tubes. The NMR tubes were sealed with Teflon plugs and stored in a desiccator under a slightly positive pressure of argon. Quantitative ^1H NMR spectra were acquired for all samples immediately after incubation, after 6 h and after 24 h. When the reaction rate between thiol and complex was very slow, the reaction was monitored up to 200 h at which point detectable thiol autooxidation could be observed in control samples.

2.8. Yeast growth

The *S. cerevisiae* strain LL20 (*MATαhis3–11, 15, leu-2, 112*) obtained from J. Huberman at Roswell Park Cancer Institute was used. Yeast were grown and maintained at 30 °C on yeast extract/peptone/dextrose (YPD) plates, and experiments were carried out in minimal salts media. The minimal medium used was yeast nitrogen base (Difco) with added histidine and leucine (5 mg/mL) and 2% dextrose (Fisher Scientific) buffered to pH 6.5 with 100 mM tris-succinate at 30 °C as previously described [38–40]. Single colonies were resuspended into 5 mL of YPD liquid media for overnight growth. A 1:40 dilution was made into minimal medium, grown overnight at 30 °C, kept at 4 °C

and used as a stock for up to two weeks. Growth was monitored using light scattering at 600 nm (OD_{600}) [38–40]. The evening before an experiment, the stock was diluted into the medium at pH 6.5 and grown overnight to generate cells growing in log phase the following day for the experiment (1:40 to 1:80 dilution depending on cell concentration of stock). The Mo salt, free ligand or complex was added to the media before the cells at the start of the final growth period (t = 0 h in the figures). Cells were diluted into the media to obtain an OD_{600} of approximately 0.1 and growth was done in 5 mL of medium in 20×150 capped culture tubes with aeration provided by rotary shaking at approximately 200 rpm. For each experimental condition, three independent growth tubes were used and growth was measured at 3, 8 and 24 h. Each measurement was the OD_{600} of the growing culture minus the OD_{600} of the medium without cells to correct for any color of the compounds [38–40]. After the OD_{600} of each sample was measured, the pH of the medium for those conditions was determined from a pool of 0.8–1.0 mL from each of the three media samples to verify that the pH of the culture medium was not changing with time. $VOSO_4$ or KVO_3 were routinely added to the media of separate control cultures to demonstrate that metal complexes could inhibit the growth of yeast in each experiment. However, from pH 4–5 the $[VO_2(dipic\text{-}OH)]^-$ complex is a much better inhibitor [40]. Statistical significance was determined using a one way ANOVA with Dunnett's multiple means test. Data obtained from cultures containing metal compounds (Mo or the vanadium control) were compared to that obtained from the control cultures with no additions taken at the same time. Significance was defined as $p \leqslant 0.05$ compared to control.

3. Results and discussion

3.1. X-ray crystallographic characterization of $[MoO_2(Me_2NO)_2]$ (2)

The coordination environment of Mo in complex **2**, shown in Fig. 1, contains structural features that are nearly identical to those found in the crystal structures of its congeners, **1** [17] and **3** [16]. Complex **2** crystallizes in the centrosymmetric $P2_1/c$ space group with the hydroxylamido ligands coordinated in a *cis*-fashion (metric parameters are given in Table 2). The overall Mo coordination environment can be described as a distorted pentagonal pyramid (with an apical oxo group) or, if the hydroxylamine is considered to be a "monodentate" ligand, a distorted tetrahedron. The Mo–O_{oxo} bond lengths of 1.70 Å are quite typical for Mo(VI) compounds [41]. The Mo–O_{HA} and the Mo–N bond lengths of 1.95 and 2.14 Å, respectively, are similar to those found in **1** [17] and **3** [16] as are the N–Mo–O_{HA} bite angles of 40°.

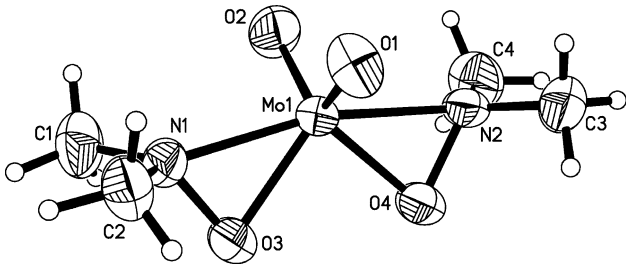

Fig. 1. The X-ray crystallographic structure and numbering scheme is shown for $[MoO_2(Me_2NO)_2]$ (**2**). The ellipsoids are drawn at the 50% probability level.

Table 2
Bond lengths (Å) and angles (°) for $[MoO_2(Me_2NO)_2]$ (**2**)

Mo(1)–O(1)	1.699(4)
Mo(1)–O(2)	1.714(3)
Mo(1)–O(3)	1.957(3)
Mo(1)–O(4)	1.957(3)
Mo(1)–N(1)	2.127(4)
Mo(1)–N(2)	2.146(4)
O(3)–N(1)	1.416(5)
O(4)–N(2)	1.425(5)
N(1)–C(2)	1.466(6)
N(1)–C(1)	1.470(6)
N(2)–C(4)	1.455(6)
N(2)–C(3)	1.480(6)
O(1)–Mo(1)–O(2)	116.03(18)
O(1)–Mo(1)–O(3)	113.11(17)
O(2)–Mo(1)–O(3)	113.62(17)
O(1)–Mo(1)–O(4)	110.71(17)
O(2)–Mo(1)–O(4)	113.77(19)
O(3)–Mo(1)–O(4)	85.91(14)
O(1)–Mo(1)–N(1)	94.32(16)
O(2)–Mo(1)–N(1)	94.31(16)
O(3)–Mo(1)–N(1)	40.32(14)
O(4)–Mo(1)–N(1)	126.21(14)
O(1)–Mo(1)–N(2)	92.66(17)
O(2)–Mo(1)–N(2)	92.95(17)
O(3)–Mo(1)–N(2)	126.22(14)
O(4)–Mo(1)–N(2)	40.33(14)
N(1)–Mo(1)–N(2)	166.54(15)
N(1)–O(3)–Mo(1)	76.3(2)
N(2)–O(4)–Mo(1)	77.0(2)
O(3)–N(1)–C(2)	110.6(4)
O(3)–N(1)–C(1)	111.8(4)
C(2)–N(1)–C(1)	113.1(4)
O(3)–N(1)–Mo(1)	63.37(19)
C(2)–N(1)–Mo(1)	122.9(3)
C(1)–N(1)–Mo(1)	121.7(3)
O(4)–N(2)–C(4)	110.5(4)
O(4)–N(2)–C(3)	110.6(4)
C(4)–N(2)–C(3)	114.8(4)
O(4)–N(2)–Mo(1)	62.70(19)
C(4)–N(2)–Mo(1)	121.1(4)
C(3)–N(2)–Mo(1)	122.1(3)

3.2. NMR spectroscopic studies

3.2.1. Description of the three environments for solution studies

The objective with solution studies is to determine if the existence of the Mo-hydroxylamido complex bears any relationship with the observed growth effects on yeast. Proper consideration requires that speciation studies be investigated in three different environments to satisfy both chemists and biologists. These conditions are low ionic strength, high ionic strength and yeast growth media. Chemists characterize compound speciation under well-defined conditions (e.g., no other complicating additives and constant ionic strength) [42]. Biologists prefer consideration of the speciation directly in the biological system in question in order to investigate the possibility that additional complexes form between the media components and the metal ion or the Mo complexes. Although studies in yeast media reflect the fundamental properties of the compounds and can determine whether new complexes form, the formation constants cannot be determined properly unless controlled conditions are used.

3.2.2. Solution studies at varying pH values

^{1}H NMR studies were first carried out at varying pH values in D_2O at low ionic strength for **1**–**3**. Initially, the solutions were investigated immediately after preparation because of the potential for these complexes to undergo redox chemistry. However, time-dependent studies showed that samples did not change over 24 h and that solutions prepared from pure complex or ligand and molybdate were found to give indistinguishable spectra in the pH range investigated (pH 3–7). The ^{1}H NMR spectra of solutions containing a 1:2 ratio of Mo to ligand are shown in Fig. 2 for **2** from pH 3 to 7. A bell-shaped curve (vide infra) showed that the highest concentration of the complex occurs between pH 4.5 and 5.5.

3.2.3. Determination of apparent formation constant

After examining the pH stability curve for the complex, a concentration study at pH 5.7–5.8 was done at constant high ionic strength (0.40 M KCl). Eukaryotic cells have different concentrations of the most important ions: 130–400 mM K^+, 10–50 mM Na^+, 4–150 mM Cl^-, and approximately 12 mM HCO_3^-. The fluids surrounding the cells, such as blood, may contain 4–20 mM K^+, 145–440 mM Na^+, 116–560 mM Cl^-, 2–10 mM Ca^{2+}, 2 mM Mg^{2+} and 30 mM HCO_3^- [43]. However, in order to determine apparent formation constants it is necessary to carry out the experiments in solutions containing only one ionic species at a constant concentration. The molybdate concentration was chosen in the mM range, in part because this concentration range is well suited for speciation studies and because it is relevant to the yeast studies reported in this work as described above. Oligomeric oxomolybdates form in the mM concentration range [37] with heptamolybdate being the major species present. The stoichiometry for complex **2** was confirmed to be 1:2 as shown by the linear relationship for the reaction (1) as shown in Fig. 3. The β for the reaction is defined in (2) and is obtained as the slope from Fig. 3 to be 15.3 ± 0.1:

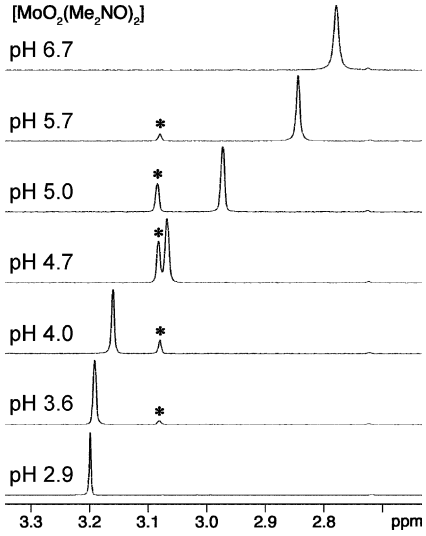

Fig. 2. ^{1}H NMR spectra of 2.5 mM $[MoO_2(Me_2NO)_2]$ (**2**) (complex is denoted by a ∗; the other peak is free ligand by an L) are recorded as a function of pH. The free ligand signal at 3.20 ± 0.01 ppm at pH 2.9 shifts upon deprotonation to 2.76 ± 0.01 ppm at pH 6.7.

$$MoO_4^{2-} + 2Me_2NOH + 2H^+ \rightleftharpoons [MoO_2(Me_2NO)_2] + 2H_2O \quad (1)$$

$$\beta = [MoO_2(Me_2NO)_2]/[MoO_4^{2-}][Me_2NOH]^2[H^+]^2 \quad (2)$$

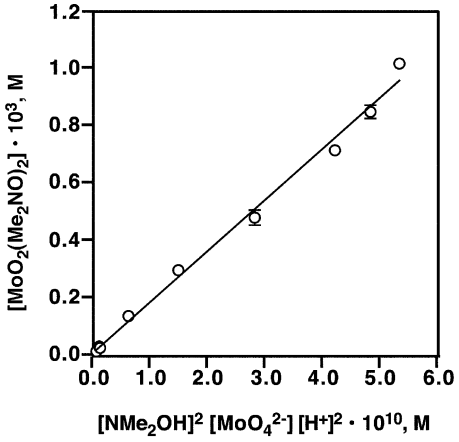

Fig. 3. The concentration of $[MoO_2(Me_2NO)_2]$ (**2**) is plotted as a function of $[MoO_4^{2-}][Me_2NOH]^2[H^+]_2$. The straight line indicates a 1:2 stoichiometry of Mo and ligand in the complex. All points are averages of three independent experiments, and error bars represent three standard deviations.

The formation constants were determined in 0.40 M KCl and then used to calculate the speciation diagram of 2.5 mM $[MoO_2(Me_2NO)_2]$ (or a 1:2 ratio of molybdate to ligand), Fig. 4(a), and for a system with 5.0 mM molybdate and 20 mM Me_2NOH, Fig. 4(b). The aqueous molybdate speciation and formation of heptaoxomolybdate was assumed as described previously [37]. The speciation at 0.40 M KCl resembles the speciation in cells as described above. A 10-fold increase in the pH-dependent formation constant was observed in pure water compared to that described in 0.40 M KCl.

When similar studies were carried out with **1** and **3**, both showed a bell curve stability pattern. More of complex **1** was formed over a wider pH range (pH 4–6.5) compared to that of **2**. Complex **3** was also very similar to **2** and gave a bell curve with a maximum between pH 4 and 5, slightly shifted from that of the corresponding Me_2NOH complex. Presumably the bell curve reflects the availability of the precursors for the reaction shown in Eq. (3); the concentration of complex decreases when the respective components are depleted. In a previous study, we showed that the formation of vanadium(V) complexes from vanadate and triethanolamine derivatives also gave a bell curve with the maximum complex concentration found at the pH defined by $(pK_{a,Vi} + pK_{a,amine})/2$ [44]. Since the Mo-hydroxylamido complexes also follow a bell curve pattern and involve complex formation between an oxoanion and a neutral amine, reaction (3) was considered from this point of view. The most prevalent mononuclear molybdate form in this pH range is $HMoO_4^-$ with a pK_a value of 3.6. This species forms a complex with Me_2NOH, MeHNOH, and Et_2NOH. The pK_a values for these ligands can be determined from their ^1H NMR chemical shifts and by extrapolating from known data (for the MeHNOH and Me_2NOH ligands) at lower ionic strength [45]. For Me_2NOH, our pK_a value of 5.4, determined by ^1H NMR, was in exact agreement with the reported value [45] after the Davies equation was used to adjust for the ionic strength. The pK_a values for MeHNOH (6.1), and Et_2NOH (5.7) are greater than that of Me_2NOH and the observation that both these ligands form lesser amounts of complex may be explained by the fact that these ligands have pK_a values that are more than 2 pH units away from that of the $HMoO_4^-$ ion

$$MoO_4^{2-} + 2RR'NOH + 2H^+ \rightleftharpoons [MoO_2(RR'NO)_2] + 2H_2O \quad (3)$$

These speciation studies provide the detailed characterization of the speciation of this class of compounds at constant ionic strength. Once a series of studies at one concentration of complex has been measured in yeast media, these data and the formation constants from the 0.4 M KCl study can be used to extrapolate the concentration of the intact complex in the yeast media.

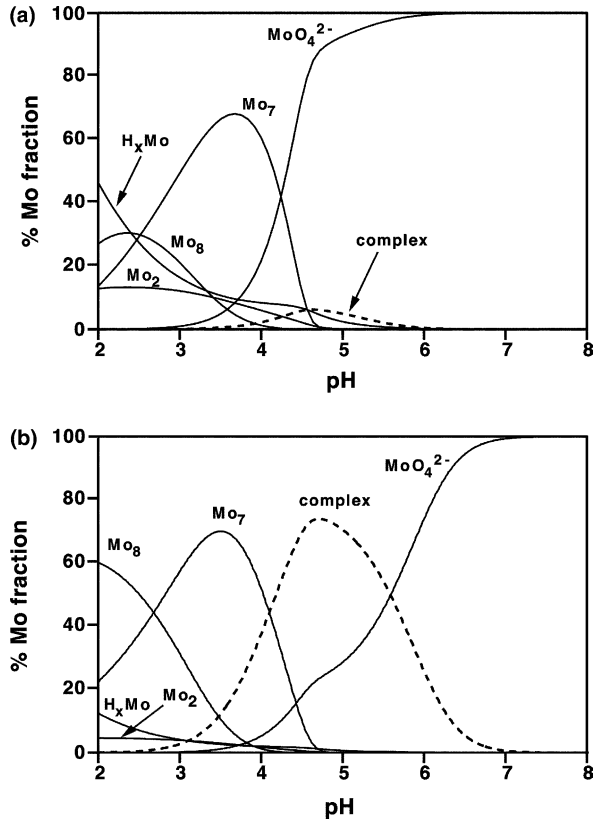

Fig. 4. The calculated speciation diagram for a system containing 2.5 mM molybdate and 5.0 mM Me_2NOH (a) and for a system containing 5 mM molybdate and 20 mM Me_2NOH (b) using formation constants determined in the presence of 0.40 M KCl. The $[HMoO_4]^-$ and the $[Mo(OH)_6]$ species are collectively referred to as "H_xMo"; the $[HMo_2O_7]^-$ species as "Mo_2"; the $[Mo_7O_{24}]^{6-}$, $[HMo_7O_{24}]^{5-}$, $[H_2Mo_7O_{24}]^{4-}$, species as "Mo_7"; and the $[Mo_8O_{26}]^{4-}$ species as "Mo_8".

3.2.4. Determination of complexes in growth media

The studies in D_2O with 0.40 M KCl provide information on the properties of these complexes. The general stability of these complexes was also determined in yeast media to eliminate the possibility that newly formed complexes with media components are responsible for the growth effects observed. Difco minimal salts media (Yeast Nitrogen Base) has approximately 50 mM of mixed salts with cations (NH_4^+, K^+, Mg^{2+} and Na^+) [3] and anions (SO_4^{2-}, PO_4^{3-}, and Cl^-) [3] as well as added histidine and leucine (5 mg/mL), 2% dextrose and is buffered to pH 6.5 with 100 mM tris-succinate.

We show the spectra of a solution at 2.5 mM $[MoO_2(Me_2NO)_2]$ at pH 5.0 in D_2O, at pH 5.0 in the presence of 0.40 M KCl in D_2O and pH 5.0 in the yeast media in Fig. 5. Due to the different environments slight shifts are observed for the signals arising from the complex ('*') and free ligand ("L") as shown for $[MoO_2(Me_2NO)_2]$

[3] The ions are listed in order from highest to lowest concentration.

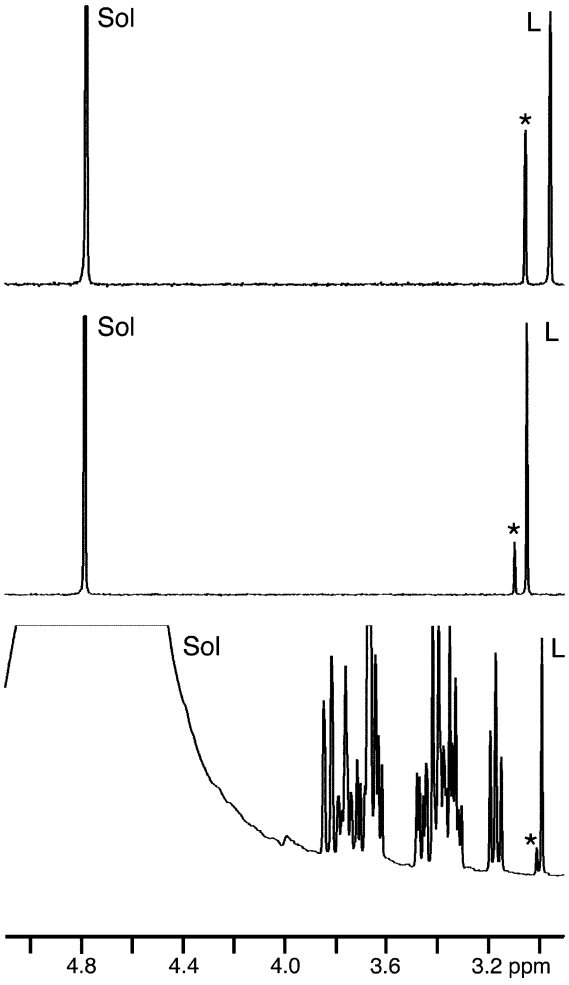

Fig. 5. Representative ^{1}H NMR spectra of 2.5 mM solutions of $[MoO_2(Me_2NO)_2]$ at pH 5 in D_2O (a), at pH 5 in D_2O/0.40M KCl (b) and at pH 5 in yeast media (c). Labels for the peaks are as follows: intact complex ("*"), free ligand ("L") and solvent ("Sol").

and Me_2NOH in Fig. 5. As a result of these differences, the ligand and complex concentrations can be determined with greater accuracy and precision in samples with D_2O (see also Table 3 below). Studies carried out in D_2O set the stage for further studies under controlled conditions to characterize the speciation, and to ultimately determine how much of the complex exists in media. As seen from the spectra in Fig. 5, the concentration of complex is highest in pure (low ionic strength) D_2O. The complexes under investigation are only a minor component in media. The studies in yeast media thus produce spectra with many pronounced ^{1}H NMR signals due to the H_2O solvent and the ions and buffers present in the yeast media (Fig. 5). A comparison with spectra in the media with no complex showed that no additional complexes are observed above the detection limit of the experiment. Note that the concentrations of the complexes in the yeast media are smaller than those observed in pure D_2O and approximately equal to those observed in the presence of 0.40 M KCl. The possibility that a minor very potent Mo complex forms below the detection limit is difficult to disprove. However, based on the chemical characterization of the Mo-hydroxylamido complexes in this paper and the known Mo(VI) chemistry, it is unlikely that ternary complexes of the Mo-hydroxylamido complex and media components are responsible for the observed growth inhibition effects. This conclusion is based on the fact that none of the media components have the structure associated with good ligands to Mo(VI) or as a ligand in a ternary Mo-hydroxylamido-ligand complex.

In Table 3, complex and ligand concentrations were determined in D_2O with 0.40 M KCl and in yeast media to demonstrate the accuracy of our D_2O model system for the 2.5 mM study. Lower accuracy and precision are obtained in studies directly in media compared to those in D_2O. Every entry in Table 3 reflects the result of three independent NMR samples prepared under the specified conditions. In spectra where no Mo complex is observed above the detection limit (pH 3 and pH 7 for compounds **1**–**3**) or where no ligand is observed above the detection limit (all pH values for compound **4**), the error represents the minimum amount of complex or ligand that has been observed in such solutions. The results shown in Table 3 indicate that none of the three hydroxylamido complexes remain intact at observable concentrations at pH 3 because they have mostly hydrolyzed to free ligand and oxomolybdates. These complexes exist at pH 5 and a small, but a significant fraction of the $[MoO_2(MeHNO)_2]$ complex remains intact at pH 6. None of the samples indicated the presence of any intact complex at pH 7. In contrast, the $[Mo(NO)(H_2NO)(H_2O)(dipic)]$ complex (**4**) remains intact over the entire pH range examined in D_2O, in D_2O with 0.40 M KCl and in media (pH 3–7); in no spectrum was any free ligand observable for this compound.

3.3. Lability of Mo complexes

The hydrolysis and ligand exchange of the Mo complexes were probed with ^{1}H NMR spectroscopy by using dilution and variable temperature experiments. As predicted from Eqs. (1)–(3), a concentrated solution of complex contains different relative amounts of complex and free ligand than that of a 10-fold diluted sample at the same pH value. Thus, measuring the ^{1}H NMR spectrum of the complex sample, diluting the sample and rapidly measuring the ^{1}H NMR spectrum of this sample will show whether equilibration has taken place. In a representative dilution experiment at pH 5.2, the added complex (25 mM) was found to hydrolyze to give a spectrum that is indistinguishable from a freshly prepared dilute sample (2.5 mM) documenting that the reaction is complete in less than 5 min (data not shown). A variable-temperature ^{1}H NMR experiment from 25–80 °C

Table 3
Amounts of compound present in 2.5 mM solutions of complexes **1**–**4** in D_2O, D_2O/0.40 M KCl, and H_2O/yeast media at pH 3.0, 5.0, 6.0 and 7.0[a] as determined from ^1H NMR studies

Conditions	Percent of intact complex (% ± SD)[b]			
	$[MoO_2(MeHNO)_2]$ (complex **1**)	$[MoO_2(Me_2NO)_2]$ (complex **2**)	$[MoO_2(Et_2NO)_2]$ (complex **3**)	$[Mo(NO)(H_2NO)(H_2O)(dipic)]$ (complex **4**)
D_2O, pH 3.0	NC[c]	NC[c]	NC[c]	NL[d]
D_2O/KCl, pH 3.0	NC[c]	NC[c]	NC[c]	NL[d]
Media, pH 3.0	NC[c]	NC[c]	NC[c]	NL[d]
D_2O, pH 5.0	2.3 ± 0.5	35.5 ± 0.4	11.3 ± 1.0	NL[d]
D_2O/KCl, pH 5.0	O[e]	13.2 ± 0.9	2.2 ± 0.4	NL[d]
Media, pH 5.0	O[e]	15.1 ± 0.9	1.5 ± 0.4	NL[d]
D_2O, pH 6.0	NC[c]	3.7 ± 0.4	0.6 ± 0.2	NL[d]
D_2O/KCl, pH 6.0	NC[c]	1.9 ± 0.1	NC[c]	NL[d]
Media, pH 6.0	NC[c]	2.3 ± 0.7	NC[c]	NL[d]
D_2O, pH 7.0	NC[c]	NC[c]	NC[c]	NL[d]
D_2O/KCl, pH 7.0	NC[c]	NC[c]	NC[c]	NL[d]
Media, pH 7.0	NC[c]	NC[c]	NC[c]	NL[d]

[a] For the D_2O solutions, the listed pH is the measured pH − 0.4.
[b] The value is an average of three separate, independent NMR experiments. The standard deviation of those three measurements is given as the error. Where no value is given, NC stands for No complex, NL stands for No ligand and O for overlap.
[c] No Mo-hydroxylamido complex or any other new complexes were observed in any of the independent samples. The lowest amount of complex observable in these spectra is 0.01 mM for the D_2O and D_2O/KCl experiments and 0.05 mM for the measurements in media.
[d] No free ligand or any other new complexes were observed in any of the independent samples. The lowest amount of free ligand observable in these spectra is 0.01 mM for the D_2O and D_2O/KCl experiments and 0.05 mM for the measurements in media.
[e] The expected signal arising from the complex overlaps with the signal of the free ligand.

failed to show the complex and free ligand signals approaching coalescence (data not shown) suggesting that the process is too slow to be measured on the NMR timescale in contrast to vanadium-hydroxylamido complexes [46]. Combined, these experiments document that these Mo-hydroxylamido complexes undergo ligand exchange too slowly to be examined by variable temperature ^1H NMR spectroscopy, but that the reaction is complete in a few minutes as found by the dilution experiments. These experiments show that complexes **1**–**3** can readily give up their metal ion upon entering the cell; this is in contrast to complex **4,** which is inert with regard to ligand exchange and will require some form of biotransformation before the metal ion is released.

3.4. Thiol reduction of Mo complexes

To examine the possibility of potential biotransformations of the hydroxylamido complexes in a reducing cellular environment, the reactivity of the complexes with thiols was examined. This measurement was done using an NMR assay in which the oxidation of thiol in the presence of complex was monitored as a function of time. 2-Mercaptoethanol (5 mM) in the presence of **2** (5 mM) was found to react slowly and even after 24 h only 4% of the thiol had been oxidized. A peroxomolybdenum complex, $[MoO(O_2)(H_2O)(dipic)]$ (**5**), used as a positive control, was found to react rapidly and after 24 h more than 50% of the thiol had been oxidized. Neither molybdate nor **4** showed a tendency to reduce in the presence of 2-mercaptoethanol at pH 5.0. The rates of reduction did not change significantly when changing the pH from 5 to 7. We therefore conclude that molybdate and these Mo-hydroxylamido complexes are only slowly reduced under the reducing physiological conditions of the cytoplasm partially maintained by intracellular glutathione concentrations of 10 mM [47].

These results differ from the effects reported with vanadate in yeast, since cellular vanadium(IV) appears after cells are exposed to vanadate in the yeast medium [38]. However, reactions of the thiols with the simple vanadium-hydroxylamido complexes did not result in thiol oxidation [48], and the formation of new complexes has been reported [49].

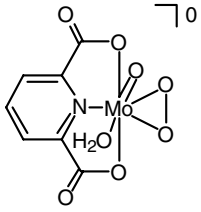

$[MoO(O_2)(H_2O)(dipic)]$ (5)

3.5. Electrochemistry

Cyclic voltammograms were recorded for 2.5–5.0 mM solutions of the complexes at pH 5 where complexes are intact. All the free ligand cyclic voltammograms gave

peaks outside the thermodynamic stability range for H_2O. Furthermore, some cathodic features observed in the cyclic voltammograms of the complexes are similar to those observed from pure ligands. Cyclic voltammograms of sodium molybdate were in agreement with previous reports [50]. Although cathodic currents were observed in the Mo complexes, none were within the thermodynamic stability range for H_2O. We conclude that complexes **1**–**4** will not undergo redox chemistry under physiological conditions unless facilitated by some biotransformation process.

3.6. Yeast growth studies

3.6.1. Effects of ligands and Mo salt

Yeast growth was monitored at varying pH values, and yeast was found to grow similarly from pH 3.0 to 7.0 (control curves in Fig. 6). To establish a baseline for comparison with the effects of metal complexes, the effects of the free ligands and molybdate on cell growth were first determined. Positive controls were done using compounds known to inhibit yeast growth at all pH values and are not shown in the figures. The most effective positive controls are vanadyl sulfate (pH 3.0), $[VO_2(dipic\text{-}OH)]^-$ (pH 5.0) [40] and vanadate (pH 6.0 and 7.0). The yeast were exposed to 10 mM of the monoalkyl- and dialkylhydroxylamine ligands at pH 3.0 (Fig. 6(a)), 5.0 (Fig. 6(b)), 6.0 (Fig. 6(c)) and 7.0 (Fig. 6(d)). At pH 3.0, none of the ligands had any effect on growth (Fig. 6(a)). At pH 5.0, the ligands have only a slight, but significant ($p < 0.0009$), effect on growth at 8 h. At pH 6 (Fig. 6(c)) and pH 7 (Fig. 6(d)) the ligands affect yeast growth differently. The monoalkylhydroxylamine (MeHNOH) ligand inhibited growth the most, the Me_2NOH ligand inhibited growth somewhat and the growth inhibition by the Et_2NOH ligand was indistinguishable from control. The observed pattern of growth inhibition by the hydroxylamine ligands follows the greater tendency of monoalkylhydroxylamines over the dialkylhydroxylamines to form radicals [27] and not the order of lipophilicity of these ligands and complexes ($Et_2NOH > Me_2NOH > MeHNOH > H_2NOH$). Since the effectiveness of ligand does not follow lipophilicity these results imply that a transport protein in the membrane is involved in the entry of the ligand into the cell.

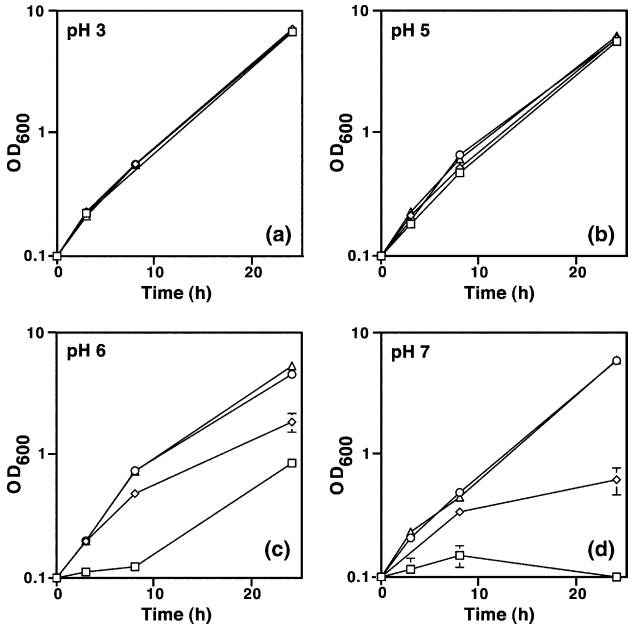

Fig. 6. Growth of yeast in the presence of 10 mM MeHNOH, Me_2NOH, and Et_2NOH at pH 3 (a), pH 5 (b), pH 6 (c) and at pH 7 (d). Control no ligand (triangle), the MeHNOH ligand (square), the Me_2NOH ligand (diamond), and the Et_2NOH ligand (circle). Points indicate the average of three measurements. The error bars represent ± SD and are mostly covered by the symbols.

The results of the corresponding treatment of yeast with $[(NH_4)_6(Mo_7O_{24}) \cdot 4H_2O]$ under similar conditions are shown in Fig. 7. Yeast studies with $Na_2MoO_4 \cdot 2H_2O$ in D_2O were indistinguishable from the yeast studies with heptamolybdate (data not shown). The salt inhibits yeast growth only at pH 3 as shown in Fig. 7(a); no substantial growth inhibition was observed at pH 5, 6, and 7 (data shown for pH 5, Fig. 7(b)). A slight, but significant ($p < 0.0009$), reduction in growth is observed at pH 5.0, similar to that seen for ligand alone, in the first 8 h. Since none of the complexes are intact at pH 3 (vide supra) and the ligands do not have any effects at this pH, any observed yeast growth inhibition at pH 3.0 is due to oxomolybdate anions. As reported previously molybdate does become cell-associated in *S. cerevisiae*, which is not true for another yeast species [6].

3.6.2. Effects of Mo complexes

Since the Et_2NOH ligand has no effect on growth, any growth inhibition caused by the Mo complex would be due *solely* to the complex and is therefore discussed

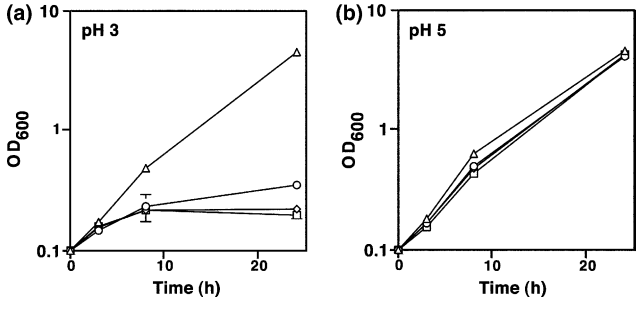

Fig. 7. Growth of yeast in the presence of various concentrations of molybdate is shown at pH 3 (a) and at pH 5 (b). Growth conditions are described in the experimental section. Control, 0 mM molybdate (triangle), 1.0 mM molybdate (circle), 2.5 mM molybdate (diamond), and 5.0 mM molybdate (square). Points indicate the average of three measurements. Error bars represent ± SD and are mostly covered by the symbols.

first. The possibility that new Mo complexes formed when the complex was added to the media is not likely, as discussed earlier and shown in Table 3. No new Mo complex was observed above the detection limit in the presence of media components at 2.5 mM concentration of complex as expected given that no growth media components are effective ligands for Mo(VI). The results from the yeast studies of complex **3** at pH 3.0, 5.0, and 6.0 are shown in Fig. 8(a)–(c). The data show, that solutions of **3** inhibit yeast growth at pH 3 (Fig. 8(a)), at pH 5 (Fig. 8(b)) and pH 6 (Fig. 8(c)) for the 2.5 and 5.0 mM concentrations. Only slight growth inhibition at 24 h is observed for any Mo complex concentration at pH 7; and only the positive control substantially inhibited growth at this pH (data not shown). Combining the data in Fig. 8 with the fact that complex **3** is unstable at pH 3, the growth inhibition observed at pH 3 is attributed to the oxomolybdate anion forming at acidic pH. Because ligand or molybdate alone do not cause growth inhibition, the observed growth inhibition at pH 5 and 6 shown in Fig. 8(b) and (C) should be attributed to the remaining intact complex as predicted from the equilibrium reaction described in this paper. Given the detection limit of the NMR experiment, our results imply that intact complex **3** is a rather potent inhibitor of yeast growth, showing an effect at the 50–100 micromolar level.

Corresponding studies were carried out with the Mo complex of *N*,*N*-dimethylhydroxylamine (Me_2NOH) as shown in Fig. 9(a)–(c). Since 10 mM Me_2NOH is inhibitory at pH 7, the study at this pH is not shown. The data in Fig. 9(a)–(c) show that solutions of complex **2** inhibit yeast growth at pH 3 (Fig. 9(a)), at pH 5 (Fig. 9(b)) and pH 6 (Fig. 9(c)). Growth inhibition at pH 3 is consistent with the effect of the oxomolybdate anions (vide supra and Fig. 7). Complex **2** inhibits growth at pH 5.0 and 6.0 as complex **3** does, but complex **2** is more potent at pH 5. Although complexes **2** and **3** are labile and undergo ligand exchange in the yeast media, a small fraction of the complex remains intact as shown in the speciation calculation for complex **2** at 2.5 mM (Fig. 4(a)). Growth inhibition is observed at the pH values where some intact complex exists and in this case can be detected in the media.

The effects of complex **1** were also determined, but since the MeHNOH ligand inhibits at pH 6 and 7, the

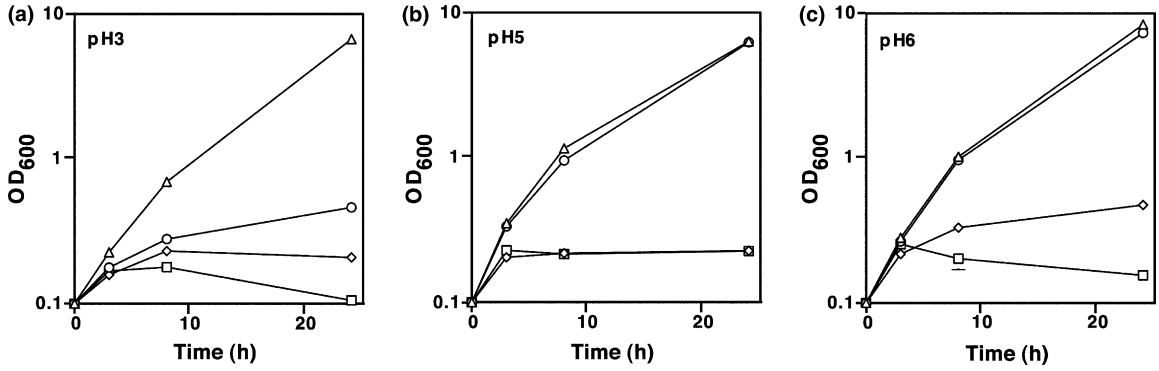

Fig. 8. Growth of yeast in the presence of $[MoO_2(Et_2NO)_2]$ (**3**) is shown at pH 3 (a), 5 (b), and 6 (c). The description of growth conditions, the symbols for different concentrations of metal compound and the use of error bars in this experiment for complex **3** are the same as given in the legend for Fig. 7.

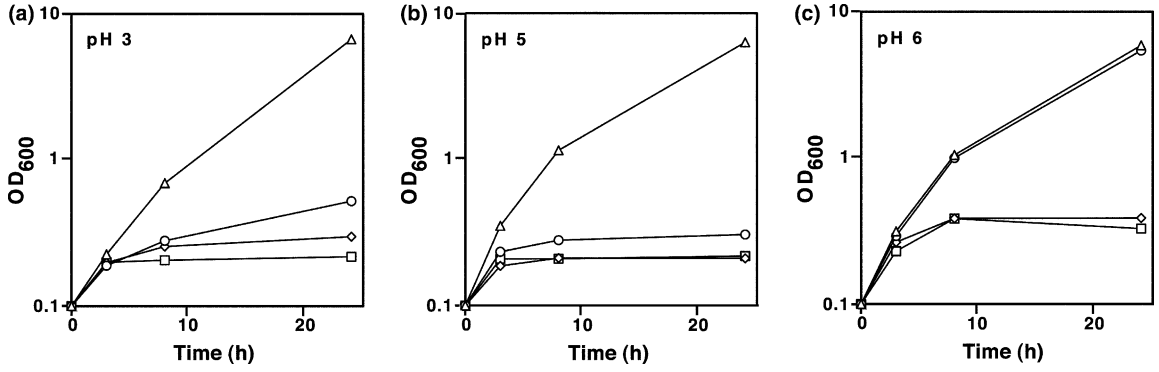

Fig. 9. Growth of yeast in the presence of $[MoO_2(Me_2NO)_2]$ (**2**) is shown at pH 3 (a), 5 (b), and 6 (c). The description of growth conditions, the symbols for different concentrations of metal compound and the use of error bars in this experiment for complex **2** are the same as given in the legend for Fig. 7.

data is only shown for the studies at pH 3 and 5 (Fig. 10(a) and (b)). The inhibition of growth by solutions of complex **1** at pH 3.0 can again be attributed to the free Mo salt as this complex is not stable at this pH. At pH 5.0, the mixture of complex and free ligand/oxomolybdate was observed to significantly ($p < 0.0009$) lower the growth at early time points, but by the 24 h time point the growth yield is indistinguishable from control. This is the only complex in which growth inhibition at 8 h appears to be greater than that seen with ligand alone. Note that the decreased yeast growth at the early points of the pH 5 study is much greater than that observed for the ligand (Fig. 6(b)) or salt (Fig. 7(b)). Since this Mo complex is detectable at pH 5 (Table 3) while other complexes are not, we attribute the observed effect to the Mo complex. However, at pH 6 and 7 a similar conclusion is circumspect, in part because the ligand inhibits and in part because at these pH values very little complex, if any, remains intact.

The effects of these labile Mo-hydroxylamido complexes on yeast were compared to a hydrolytically stable, but structurally related complex. Molybdate reacts with the H_2NOH, in the presence of chelating ligands, to form complexes with both a coordinated nitrosyl and a coordinated hydroxylamido ligand. An example of such a complex is $[Mo(NO)(H_2NO)(H_2O)(dipic)]$ (**4**) [30]. This complex distinguishes itself from the other hydroxylamido complexes investigated in this study by remaining hydrolytically intact over the entire pH range investigated. The effect of this complex on yeast growth was determined at 1, 2.5 and 5 mM at pH 3.0, 5.0, 6.0 and 7.0. Data for the studies at pH 3.0 and 6.0 are shown in Fig. 11(a) and (b), respectively; the data from the pH 5 and 7 studies are indistinguishable from the pH 6.0 data and are not shown. Little growth inhibition was observed over the entire pH range at all time points, with the most inhibition seen for early times at pH 3.0. However, this slight growth inhibition was sometimes significant at the $p < 0.05$ to $p < 0.0001$ level. This is the only Mo complex we investigated that did not substantially inhibit growth at pH 3 (Fig. 11(a)). Since molybdate is found to inhibit growth at pH 3 even at 1 mM (Fig. 7(a)) the lack of inhibition by complex **4** suggests that this complex remains intact at pH 3. These results are consistent with this hydrolytically stable complex protecting the cell at pH values where aqueous Mo ions or ligands inhibit growth.

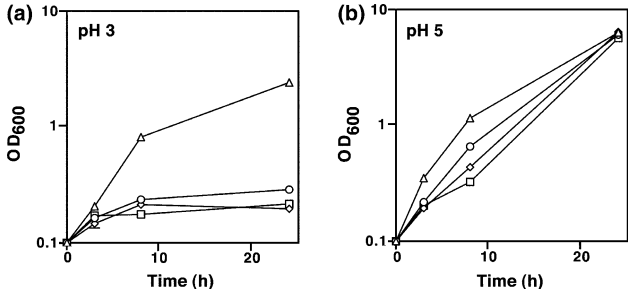

Fig. 10. Growth of yeast in the presence of $[MoO_2(MeHNO)_2]$ (**1**) is shown at pH 3 (a) and 5 (b). The description of growth conditions, symbols for different concentrations of metal compound and the use of error bars in this experiment for complex **1** are the same as given in the legend for Fig. 7.

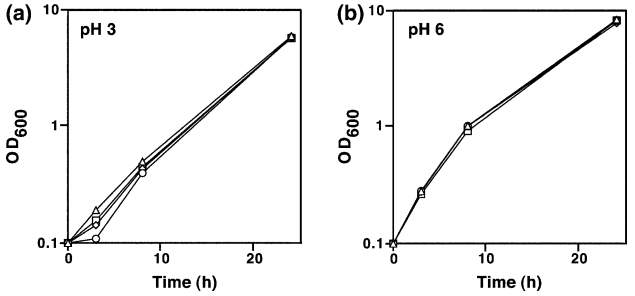

Fig. 11. Growth of yeast in the presence of $[Mo(NO)(H_2NO)(H_2O)(dipic)]$ (**4**) is shown at pH 3 (a) and 5 (b). The description of growth conditions, the symbols for different concentrations of metal compound and the error bars used in this experiment for complex **4** are the same as those given in Fig. 7.

Free metal ions are not believed to exist in the cell [51]. When a free metal ion enters the cell it can bind to multiple cellular components, many of which could keep the metal ions from interacting with critical cellular components. While neither ligand nor molybdate alone affected yeast growth, a Mo complex could inhibit the growth of yeast by selectively releasing the metal ion to bind to a component of the cell critical for growth.

Alternatively, the Mo complexes could potentially inhibit growth by formation of nitric oxide (NO). Mo-hydroxylamido complexes can serve as precursors for intracellular NO. Indeed, metal nitrosyl complexes have been postulated as potential NO delivery agents [52–56]. In contrast to the Mo-hydroxylamido complexes the Mo(NO)-type complexes are very stable over a wide pH range. Given this stability, it is likely that any NO produced from the reduction of the Mo-hydroxylamido complexes under physiological conditions will remain bound to the molybdenum and will not affect yeast growth unless facilitated by some biotransformation. The inhibition efficacy of the complexes observed in this work is: **2** > **3** > **1** ≫ **4**. The inert Mo compound is the least effective at inhibiting yeast growth while the Mo-dimethylhydroxylamido complex is the most effective. Interestingly, this order does not follow the lipophilicity of these compounds and presumably reflects that these compounds, similarly to the ligands discussed above, enter the cell through a protein transport channel.

4. Summary

The solid-state characterization of complex **2** is described and combined with the aqueous speciation of

this simple complex and other related Mo-hydroxylamido complexes. All of these complexes exist in aqueous solution in the pH range 4–6, while a related nitrosyl complex was hydrolytically stable over the entire pH range examined (pH 2–8). The Mo-hydroxylamido complexes are labile and undergo ligand exchange much like the corresponding vanadium-hydroxylamido complexes. The effects of 1.0, 2.5 and 5.0 mM of complexes **1**–**4** on yeast at pH 3.0, 5.0, 6.0 and 7.0 were determined and compared with the effects of free ligand and molybdate. Complexes **1**, **2** and **3** were found to inhibit growth at pH 3.0, which was attributed to the major oligomeric molybdate species that forms after the complexes hydrolyze. At pH 5.0 and 6.0 complexes **2** and **3** inhibited growth. Because neither ligand nor molybdate inhibited growth significantly at these pH values, the inhibition could be attributed to some intact complex in solution. Since the hydrolytically stable complex **4** showed little or no effect on yeast growth over the entire pH range, we conclude that some complexed Mo has no effect on growth inhibition. The inhibition efficacy of the complexes is: $\mathbf{2} > \mathbf{3} > \mathbf{1} \gg \mathbf{4}$. The studies have shown that even when complexes can undergo ligand exchange, their effects on growth do correlate with the presence of some level of intact complex in the growth media.

Acknowledgement

D.C.C. and G.R.W. thank the Institute for General Medicine at the National Institutes of Health for funding this work. We thank Prof. C. Michael Elliot and Mr. Jeremy Nelson for assistance with the electrochemical studies.

References

[1] F.H. Nielsen, in: M.E. Shils, J.A. Olson, H. Shike, A.C. Ross (Eds.), Ultratrace Minerals, Lippincot Williams and Wilkins, Baltimore, USA, 1999, Ch. 16.
[2] J.G. Hardman, L.E. Limbird, P.B. Molinoff, R.W. Ruddon (Eds.), Goodman and Gilman's The Pharmacological Basis of Therapeutics, McGraw-Hill, New York, 1996.
[3] A.T. Ozcelikay, D.J. Becker, L.N. Ongemba, A.-M. Pottier, J.-C. Henuin, S.M. Brichard, Am. Phys. Soc. (1996) E344–E352.
[4] B.A. Reul, D.J. Becker, L.N. Ongemba, C.J. Bailey, J.C. Henquin, S.M. Brichard, J. Endocrinol. 155 (1997) 55–64.
[5] C. Fillat, J.E. Rodriguez-Gil, J.J. Guinovart, Biochem. J. 282 (1992) 659–663.
[6] V.S. Pingale, S.P. Kale, B. Sonali, R.L. Deopurkar, V.B. Rale, Lett. Appl. Microbiol. 16 (1993) 101–103.
[7] L.H. Doerrer, J.R. Galsworthy, M.L.H. Green, M.A. Leech, M. Muller, J. Chem. Soc., Dalton Trans. (1998) 3191–3194.
[8] S.F. Gheller, T.W. Hambley, P.R. Traill, R.T.C. Brownlee, M.J. O'Connor, M.R. Snow, A.G. Wedd, Aust. J. Chem. 35 (1982) 2183–2191.
[9] S.F. Gheller, W.E. Newton, L.P. de Majid, J.R. Bradbury, F.A. Schultz, Inorg. Chem. 27 (1988) 359–366.
[10] M. Hahn, K. Wieghardt, W. Swiridoff, J. Weiss, Inorg. Chim. Acta 89 (1984) L31–L32.
[11] E. Hofer, W. Holzbach, K. Wieghardt, Angew. Chem. Int., Ed. Engl. 20 (1981) 282–283.
[12] R. Mattes, H. Scholand, U. Mikloweit, V. Schrenk, Z. Naturforsch. B42 (1987) 599–604.
[13] R. Mattes, H. Scholand, U. Mikloweit, V. Schrenk, Chem. Ber. 120 (1987) 783–787.
[14] R. Mattes, H. Scholand, U. Mikloweit, V. Schrenk, Z. Naturforsch. B42 (1987) 589–598.
[15] M. Minelli, J.H. Enemark, K. Wieghardt, M. Hahn, Inorg. Chem. 22 (1983) 3952–3953.
[16] L. Saussine, H. Mimoun, A. Mitschler, J. Fisher, Nouv. J. Chim. 4 (1980) 235–237.
[17] K. Wieghardt, W. Holzbach, J. Weiss, B. Nuber, B. Prikner, Angew. Chem. Int., Ed. Engl. 18 (1979) 548–549.
[18] K. Wieghardt, E. Hofer, W. Holzbach, B. Nuber, J. Weiss, Inorg. Chem. 19 (1980) 2927–2932.
[19] K. Wieghardt, W. Holzbach, J. Weiss, Inorg. Chem. 20 (1981) 3436–3439.
[20] K. Wieghardt, W. Holzbach, E. Hofer, J. Weiss, Inorg. Chem. 20 (1981) 343–348.
[21] K. Wieghardt, W. Holzbach, E. Hofer, J. Weiss, Chem. Ber. 114 (1981) 2700–2712.
[22] K. Wieghardt, M. Hahn, J. Weiss, W. Swiridoff, Z. Anorg. Allg. Chem. 492 (1982) 164–174.
[23] P.C. Paul, S.J. Angus-Dunne, R.J. Batchelor, F.W.B. Einstein, A.S. Tracey, Can. J. Chem. 75 (1997) 429–440.
[24] D. Rehder, K. Wieghardt, Z. Naturforsch. 36b (1981) 1251–1254.
[25] C. Weidemann, W. Priebsch, D. Rehder, Chem. Ber. 122 (1989) 235–243.
[26] E.I. Stiefel, in: G. Wilkinson Sir, R.D. Gillard, J.A. McCleverty (Eds.), Molybdenum(VI), Pergamon Press, New York, 1987, pp. 1375–1420.
[27] K. Wieghardt, Adv. Inorg. Bioinorg. Mech. 3 (1984) 213–274.
[28] J.H. Enemark, R.D. Feltham, Coord. Chem. Rev. 13 (1974) 339–406.
[29] L. Yang, A. La Cour, O.P. Anderson, D.C. Crans, Inorg. Chem. 41 (2002) 6322–6331.
[30] K. Wieghardt, W. Holzbach, B. Nuber, J. Weiss, Chem. Ber. 113 (1980) 629–638.
[31] D. Westlake, R. Kergoat, J.E. Guerchais, C. R. Seances Acad. Sci. 280C (1975) 113–115.
[32] G.M. Sheldrick, SADABS (a Program for Siemens Area Detection Absorption Correction) (2000).
[33] G.M. Sheldrick, SHELXTL, Siemens Analytical X-ray Diffraction, Siemens, Madison, WI, 1996.
[34] H. Irving, M.G. Miles, L.D. Pettit, Anal. Chim. Acta 38 (1967) 475–488.
[35] P.K. Glasoe, F.A. Long, J. Phys. Chem 64 (1960) 188–190.
[36] P. Gans, A. Sabatini, A. Vacca, HySS (Hyperquad Simulation and Speciation), Protonic Software (1998).
[37] J.J. Cruywagen, Inorg. Chem. 19 (1980) 552–554.
[38] G.R. Willsky, D.A. White, B.C. McCabe, J. Biol. Chem. 259 (1984) 13273–13281.
[39] G.R. Willsky, J.O. Leung, P.V. Offermann Jr., E.K. Plotnick, S.F. Dosch, J. Bacteriol. 164 (1985) 611–617.
[40] D.C. Crans, L. Yang, J.A. Alfano, L.-H. Chi, W. Jin, M. Mahroof-Tahir, K. Robbins, M.M. Toloue, L.K. Chan, A.J. Plante, R.Z. Grayson, G.R. Willsky, Coord. Chem. Rev. 237 (2003) 13–22.
[41] F.A. Cotton, G. Wilkinson, C.A. Murillo, M. Bochman, Advanced Inorganic Chemistry, Wiley Interscience, New York, 1999.
[42] J.C. Pessoa, I. Tomaz, T. Kiss, E. Kiss, P. Buglyo, J. Biol. Inorg. Chem. 7 (2002) 225–240.

[43] H. Lodish, A. Berk, S.L. Zipursky, P. Matsudaira, D. Baltimore, J. Darnell, Molecular Cell Biology, W.H. Freeman and Co., New York, 2000.
[44] D.C. Crans, P.K. Shin, Inorg. Chem. 27 (1988) 1797–1806.
[45] T.C. Bissot, R.W. Parry, D.H. Campbell, J. Am. Chem. Soc. 79 (1957) 796–800.
[46] A.D. Keramidas, S.M. Miller, O.P. Anderson, D.C. Crans, J. Am. Chem. Soc. 119 (1997) 8901–8915.
[47] A. Meister, M.E. Anderson, Ann. Rev. Biochem. 52 (1983) 711–760.
[48] D.C. Crans, E. Gaidamauskas, unpublished results.
[49] S. Bhattacharyya, A. Martinsson, R.J. Batchelor, F.W.B. Einstein, A.S. Tracey, Can. J. Chem. 79 (2001) 938–948.
[50] M. Pourbaix, Atlas of Electrochemical Equilibria in Aqueous Solutions, Pergamon Press, New York, 1966.
[51] T.D. Rae, P.J. Schmidt, R.A. Pufahl, V.C. Culotta, T.V. O'Halloran, Science 284 (1999) 805–808.
[52] P.C. Ford, J. Bourassa, B. Lee, I. Lorkovic, K. Miranda, L. Laverman, Coord. Chem. Rev. 171 (1998) 185–202.
[53] P.C. Ford, Int. J. Photoenergy 3 (2001) 161–169.
[54] T.W. Hayton, P. Legzdins, W.B. Sharp, Chem. Rev. 102 (2002) 935–991.
[55] G. Stochel, E. Ilkowska, M. Pawelec, A. Wanat, M. Wolak, ACH-Models Chem. 135 (1998) 847–871.
[56] A.M. English, D.E. Wilcox, Met. Ions Biol. Syst. 38 (2001) 313–350.